

The two-atom energy spectrum in a harmonic trap near a Feshbach resonance at higher partial waves

Akira Suzuki

Department of Physics, Tokyo University of Science, Tokyo, Japan 162-8601

Yi Liang and Rajat K. Bhaduri

Department of Physics and Astronomy, McMaster University, Hamilton, ON, Canada L8S 4M1

(Dated: November 10, 2018)

Two atoms in an optical lattice may be made to interact strongly at higher partial waves near a Feshbach resonance. These atoms, under appropriate constraints, could be bosonic or fermionic. The universal $l = 2$ energy spectrum for such a system, with a caveat, is presented in this paper, and checked with the spectrum obtained by direct numerical integration of the Schrödinger equation. The results reported here extend those of Yip for p -wave resonance (Phys. Rev. A **78**, 013612 (2008)), while exploring the limitations of a universal expression for the spectrum for the higher partial waves.

PACS numbers: 03.75.-b, 03.75.Ss, 34.50.-s, 37.10.Jk, 67.85.-d

I. INTRODUCTION

Normally, the scattering between two neutral atoms in higher partial waves is suppressed due to the centrifugal barrier. The situation may change, however, by sweeping a static magnetic field near a Feshbach resonance (FR) at a higher partial wave [1, 2]. In such a situation, the relative energy of the scattering atoms is at near-coincidence with the energy of a quasi-bound molecular state with a nonzero angular momentum. FR was first observed with bosons interacting in the s -state [3], and later in higher partial waves [2]. Two spin polarized fermions may interact in a relative odd- l state in a single channel ultra-cold gas, or in an even- l state when the two atoms are in distinct spin states. The single-channel p -wave FR was first observed by Regal et al. [1] between ^{40}K atoms, while the fermionic s -wave between these atoms in distinct spin states was observed by the same group a little earlier [4].

The two-particle energy spectrum in a spherical harmonic oscillator (HO) near a s -wave FR is found to be universal when the range of the interaction between the two atoms is much smaller than the average interparticle distance in the HO, i.e. the oscillator length [5, 6, 7]. Near the Feshbach resonance, this spectrum has been checked experimentally [8] in the limit of low tunneling for fermionic ^{40}K atoms in an optical trap in two distinct spin states. This is remarkable because the theoretical spectrum is obtained in a one-channel approximation, and fits the data even with the first term in the effective range expansion. More recently, Yip [9] has obtained the spectrum of two identical fermions in a HO near a p -wave FR. It is known that the p -wave FR gets split [10] between $|m_l| = 1$ and 0. Yip's calculation is for $m_l = 0$, but may be generalised for nonzero m_l . For higher partial waves, however, it was stated that the energy spectrum could not be expressed in terms of the parameters in the scattering amplitude and the oscilla-

tor constant [9, 11]. In this paper, using a method first formulated by Jonsell [6] for $l = 0$, we express the energy spectrum for the higher partial waves in terms of the scattering parameters. We examine the $l = 2$ case in detail, and compare the spectra obtained from this analytical formula with the results obtained by a numerical integration of the Schrödinger equation. Yip's assertion is justified, but only in a narrow region at resonance where the ground state energy goes to zero. The analytical formula accurately reproduces the excited state spectrum in the entire range, but is shown to be not accurate for the ground state in a narrow band across the resonance. With this exception, even though the energy spectra for $l = 1$ and $l = 2$ are extremely sensitive to the choice of the effective range parameter, we find that the levels are practically unchanged by introducing the next term in the expansion, which is shape-dependent.

In calculating the p wave spectrum, Yip used the effective range expansion for higher partial waves [12]

$$k^{2l+1} \cot \delta_l(k) = -\frac{1}{a_l} + \frac{1}{2} r_l k^2, \quad (1)$$

with $l = 1$. Note that the scattering length a_l and the effective range r_l have the dimensions of $(L)^{2l+1}$ and $(L)^{-2l+1}$ respectively. For single channel elastic scattering by a power-law potential r^{-n} , and *without any virtual transition to other channels like an excited quasi-molecular state*, a_l in Eq.(1) is only defined if $n > (2l + 3)$ [13]. For the effective range r_l to exist, the restriction is even more severe, $n > (2l + 5)$. Taking $n = 6$ for the asymptotic behaviour of the interatomic potential, we see that for $l = 1$, only a_1 exists, but not r_1 . For $l = 2$, neither a_2 , nor r_2 is defined [13, 14].

The situation changes, however, for dressed atoms near a Feshbach resonance. Consider scattering in an open channel which is coupled to a resonance in the closed channel through a spin-dependent *two-body* interaction W that depends on the relative distance r between the two atoms [15]. One part is the long range tensor inter-

action between the two dipoles that falls off as r^{-3} . The other is the spin-exchange interaction between the two valence electrons of the alkali atoms that are closer than the uncoupling distance r_u . For $r < r_u$, the nuclear and electronic spins that were otherwise coupled in an isolated atom get uncoupled due to one atom's proximity to the other atom. The resulting spin-exchange interaction has a range r_u which is smaller than the so-called van der Waals distance, a measure of the length scale for the r^{-6} potential. The coupling potential W may therefore be regarded as of shorter range than r^{-6} in cases where the spin exchange interaction is dominant.

Elimination of the closed channel results in an additional effective potential in the single-channel formalism. This effective potential, which dominates the open channel scattering near the Feshbach resonance, contains W quadratically. The effective range expansion should be valid for the higher partial waves for this short range potential, as will be discussed in the next section.

II. THE TWO-BODY PROBLEM

A. Two-channel scattering

We first recall the well-known results of two-channel scattering, following the treatment and notation of Cohen-Tannoudji [17]. The Hamiltonian H is a 2×2 matrix, with the diagonal elements H_{op} and H_{cl} , and the nondiagonal coupling given by the short range spin exchange potential W . Here $H_{op} = (-\nabla^2 + V_{op})$, with V_{op} given by the van der Waal power law potential whose asymptotic fall-off goes like r^{-6} . The closed channel Hamiltonian, in the single-resonance approximation, may be expressed as $H_{cl} = E_{res}|\phi_{res}\rangle\langle\phi_{res}|$, with the resonance energy at E_{res} .

The wave function ψ is a column matrix with two components ϕ_{op} and ϕ_{cl} . It is straightforward to show that the two-channel scattering problem may be described entirely in the open channel by a Lippman-Schwinger equation in which the incident wave is distorted by the open channel potential V_{op} , and the scattering is by the effective potential V_{eff} . More explicitly, the (relative) outgoing wave of the dressed atoms $|\phi_{op}^k\rangle$, in terms of the distorted wave $|\phi_k^+\rangle$, is given by

$$|\phi_{op}^k\rangle = |\phi_k^+\rangle + G_{op}^+(E)V_{eff}|\phi_k^+\rangle, \quad (2)$$

where

$$V_{eff} = W \frac{|\phi_{res}\rangle\langle\phi_{res}|}{E - E_{res} - \langle\phi_{res}|WG_{op}^+(E)W|\phi_{res}\rangle} W. \quad (3)$$

In the above, $G_{op}^+(E) = (E - H_{op} + i\epsilon)^{-1}$. The distorted incident wave $|\phi_k^+\rangle$ itself obeys a Lippman-Schwinger equation in which the incident wave is a plane wave, the Green's function is $(E - T + i\epsilon)^{-1}$, and the scattering potential is V_{op} . As $k \rightarrow 0$, the large- r behaviour of the first term on the RHS of Eq.(2) gives the background scattering length, and the second term yields the

energy-dependent scattering length that dominates near the Feshbach resonance. Since we have in mind partial waves $l \geq 2$, and $V_{op}(r) = -(\hbar^2/M)C_6/r^6$, the background scattering length does not exist [13, 14]. Indeed, the phase shift caused by this potential is vanishingly small for small k . This background phase shift, denoted by $\delta_l^{bg}(k)$, is given by [18]

$$\tan \delta_l^{bg}(k) = \frac{\pi}{2} 2^{-5} C_6 \frac{\Gamma(5)\Gamma(l-3/2)}{\Gamma^2(3)\Gamma(l+7/2)} |k|^3 k. \quad (4)$$

The distortion in the incident wave ϕ_k^+ for small k may therefore be neglected, and the scattering for the higher partial waves at low energies is governed by the energy-dependent short range potential V_{eff} . As usual, the energy denominator in it may be related to the Zeeman splitting due to a sweeping magnetic field, giving rise to a large variation of the scattering length a_l near FR. We may then express the flow of the energy levels as a function of the scattering length, assuming a fixed effective range r_l in the expansion (1). This we proceed to do, generalising a method first proposed by Jonsell [6] for $l = 0$. We confine our treatment to $m_l = 0$.

B. Energy spectrum in harmonic trapping

Each particle, of mass M , moves in a harmonic potential $(1/2)M\omega^2 r^2$. Making the usual transformations to relative and CM co-ordinates, $\mathbf{r} = (\mathbf{r}_1 - \mathbf{r}_2)$, and $\mathbf{R} = (\mathbf{r}_1 + \mathbf{r}_2)/2$, and their corresponding canonical momenta \mathbf{p}, \mathbf{P} , we obtain, for the noninteracting particles,

$$H_0 = \left(\frac{P^2}{2M_{cm}} + \frac{1}{2}M_{cm}\omega^2 R^2 \right) + \left(\frac{p^2}{2\mu} + \frac{1}{2}\mu\omega^2 r^2 \right), \quad (5)$$

where $M_{cm} = 2M$, $\mu = M/2$. Consider the relative motion of these two trapped particles, interacting with a short range effective potential $V_s(r)$. This is the single-channel equivalent of the potential $W^2(r)$ of Eq.(3), with the energy dependence in the denominator being absorbed in the rapidly varying scattering length parametrized by the Zeeman splitting. The two-body Schrödinger equation in each partial wave l for the radial wave function $u_l(r) = r\psi_l(r)$ with energy E_l may be expressed in dimensionless variables $x = r/(\sqrt{2}L)$, where $L = \sqrt{\hbar/(M\omega)}$, and $\eta_l = 2E_l/(\hbar\omega)$. It is given by

$$-\frac{d^2 u_l}{dx^2} + \frac{l(l+1)}{x^2} u_l + \frac{2V_s}{\hbar\omega} u_l + x^2 u_l = \eta_l u_l. \quad (6)$$

We may find the energy spectrum of the above equation without specifying the specific form of V_s by generalising a method first adopted by Jonsell [6] for $l = 0$. Let the range of the short range potential $V_s(r)$ be given by b . For $r > b$, taking $V_s = 0$, the solution of Eq.(6) is given by

$$u_l = e^{-x^2/2} \left[c'_1 x^{l+1} M\left(\frac{2l+3-\eta_l}{4}, l + \frac{3}{2}; y\right) + c'_2 x^{-l} M\left(\frac{-2l+1-\eta_l}{4}, \frac{1}{2}-l; y\right) \right], \quad (7)$$

where $y = x^2$, and $M(\alpha, \gamma; z)$ is the confluent hypergeometric function [13]. Since, for large z , $M(\alpha, \gamma; z)$ behaves as

$$M(\alpha, \gamma; z) \sim \frac{\Gamma(\gamma)}{\Gamma(\alpha)} z^{\alpha-\gamma} e^z, \quad (8)$$

the wave function behaves as

$$u_l = \left[c'_1 \frac{\Gamma(3/2+l)}{\Gamma((3+2l-\eta_l)/4)} + c'_2 \frac{\Gamma(1/2-l)}{\Gamma((1-2l-\eta_l)/4)} \right] x^{-(1+\eta_l)/2} e^{x^2/2} \quad (9)$$

for large x . In order to get a convergence solution, we have to have

$$\frac{c'_2}{c'_1} = -\frac{\Gamma(3/2+l) \Gamma((1-2l-\eta_l)/4)}{\Gamma(1/2-l) \Gamma((3+2l-\eta_l)/4)}. \quad (10)$$

Since

$$\frac{\Gamma(3/2+l)}{\Gamma(1/2-l)} = (-1)^l \left(l + \frac{1}{2} \right) \frac{[(2l-1)!!]^2}{2^{2l}}, \quad (11)$$

we obtain

$$\frac{c'_2}{c'_1} = -(-1)^l \left(l + \frac{1}{2} \right) \frac{[(2l-1)!!]^2 \Gamma((1-2l-\eta_l)/4)}{2^{2l} \Gamma((3+2l-\eta_l)/4)}. \quad (12)$$

We now need to relate this ratio to the scattering length a_l to determine the eigenvalue η_l . Note that if the range b of V_s is very small, as we approach $r \rightarrow b^+$, the oscillator potential may be neglected. *This assumption is crucial for our derivation, and is examined in some detail in Appendix A for $l = 2$.* Thus $u_l(r)$ for positive energy may be regarded as the phase-shifted scattering solution due to V_s , given by

$$u_l(r) = A_l k r [j_l(kr) - n_l(kr) \tan \delta_l], \quad (13)$$

$E_l = \hbar^2 k^2 / M$. For $r > b$, but still $\simeq 0$, $u_l(r)$ behaves as

$$u_l(r) \longrightarrow B_l r^{l+1} \left[1 + (2l+1)[(2l-1)!!]^2 \frac{\tan \delta_l}{(kr)^{2l+1}} \right], \quad (14)$$

where

$$B_l = \frac{A_l k^l}{(2l+1)!!}. \quad (15)$$

We match u_l , given by Eq.(14) with that obtained from Eq.(7) for small x . The validity of this procedure for $l = 2$ rests on the condition (24) derived in Appendix A. For

$z \rightarrow 0$, and $\gamma \neq 0$, the Kummer's functions $M(\alpha, \gamma; z)$ is unity; hence the solution given by Eq.(7) behaves as

$$u_l(x) = c'_1 x^{l+1} \left(1 + \frac{c'_2}{c'_1} x^{-2l-1} \right). \quad (16)$$

When this is matched with Eq.(14), we obtain

$$\frac{c'_2}{c'_1} = (2l+1)[(2l-1)!!]^2 \frac{\tan \delta_l}{(\sqrt{2}kL)^{2l+1}}. \quad (17)$$

Equating Eqs(12, 17), and using the effective range expansion (1), we obtain

$$\frac{1}{\sqrt{2}} \frac{\Gamma((1-2l-\eta_l)/4)}{\Gamma((3+2l-\eta_l)/4)} = (-2)^l \frac{\tilde{a}_l}{1 - \tilde{a}_l \tilde{r}_l \eta_l / 4}. \quad (18)$$

In the above, we have defined the dimensionless quantities

$$\tilde{a}_l = \frac{a_l}{L^{2l+1}}, \quad \tilde{r}_l = L^{2l-1} r_l. \quad (19)$$

If we set $l = 1$ and $L = l_r / \sqrt{2}$ following Yip [9], we recover his result, that is, his Eq.(13);

$$-\frac{l_r^3}{v} + \frac{1}{2} l_r (2c) \eta_1 = 8 \frac{\Gamma((5-\eta_1)/4)}{\Gamma((-1-\eta_1)/4)}, \quad (20)$$

where we have put $a_1 = v$ and $r_1 = 2c$. Similarly, by setting $l = 0$ in Eq.(18) we recover the spectrum of the $l = 0$ states as given by Busch [5]. Note that Eq.(18) has been obtained with no mention of any specific shape of the potential, and is valid for *any* short-range two-body potential.

III. RESULTS AND DISCUSSION

In Figs 1-3, we plot the energy spectrum given by Eq.(18) as a function of the scaled scattering length \tilde{a}_l for

$l = 0 - 2$, keeping the effective range \tilde{r}_l fixed. The same energy spectra look quite different when plotted against the inverse of the scattering length, $1/\tilde{a}_l$. For $l = 1$, we reproduce Yip's result, and do not duplicate it here. Our Fig. 4 shows the energy levels for $l = 2$, plotted as a function of $1/\tilde{a}_l$. Before discussing these spectra, we comment on the choice of the effective range parameter. For $l = 1$, Yip had set the scaled effective range $\tilde{r}_1 = -64/\sqrt{2}$ from experimental data [10]. From a theoretical point of view, to see if this may be generated by a potential whose range is much smaller than the oscillator length L , we take a square-well potential. The shape of the potential should not matter unless the shape-dependent term in the effective range expansion (proportional to k^4) affects the energy spectrum. We have verified that the spectra in Figs 1-4 remain virtually unchanged when this term is included. In the Appendix B, the analytical expressions for the scattering length and the effective range for any given partial wave are given. At a resonance, $a_l = \pm\infty$, hence it follows from Eq.(26) that $j_{l-1}(s) = 0$. Therefore, from Eq.(27) we get $r_0 = b$, $r_1 = -3/b$, and $r_2 = -15/b^3$. For Yip's choice of $r_1 L = \tilde{r}_1 = -64/\sqrt{2}$, it follows that $b/L = \tilde{b} \simeq 1/15$, fulfilling the condition that $b \ll L$. Unlike the case $l = 1$, we do not have guidance from experiment for the choice of \tilde{r}_2 , so we deduce it from the square-well potential with $\tilde{b} = 1/15, 1/30, \text{ and } 1/10$. Furthermore, we find that for the square-well example, although the scattering length is highly sensitive to the choice of the strength parameter s defined by Eq.(25), the effective range hardly changes as s is varied over a narrow range to accommodate the variation in the scattering length shown in Figs.(1-

4).

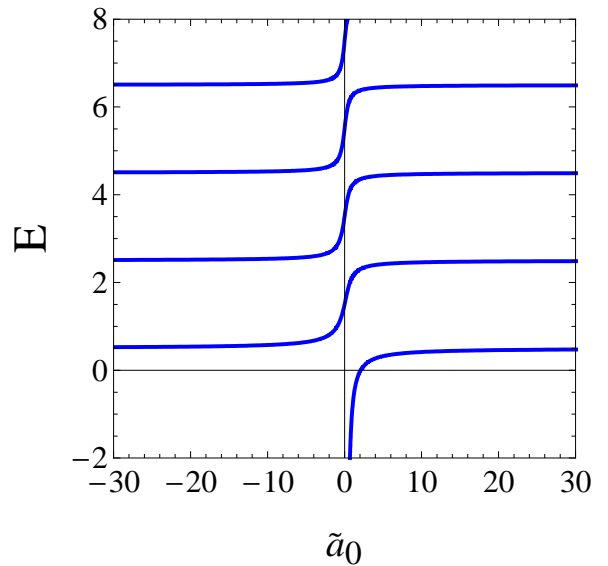


FIG. 1: (Color online) Plot of the $l = 0$ energy levels E in units of $\hbar\omega$ versus the s-wave scattering length a_0 in units of the oscillator length L . The scaled effective range is fixed at $1/15$. The plots change negligibly even for zero range.

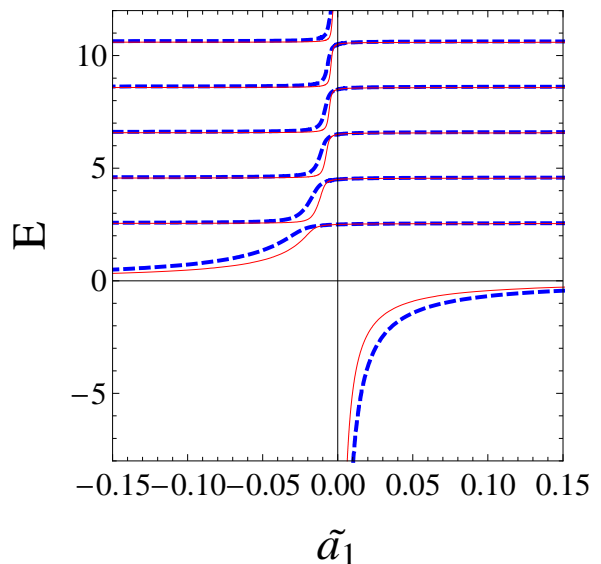


FIG. 2: (Color online) The $l = 1$ energy levels vs the scaled p -wave scattering length \tilde{a}_1 . The dashed curves are for the effective range $\tilde{r}_1 = -30$, while the continuous curves are for $\tilde{r}_1 = -45$.

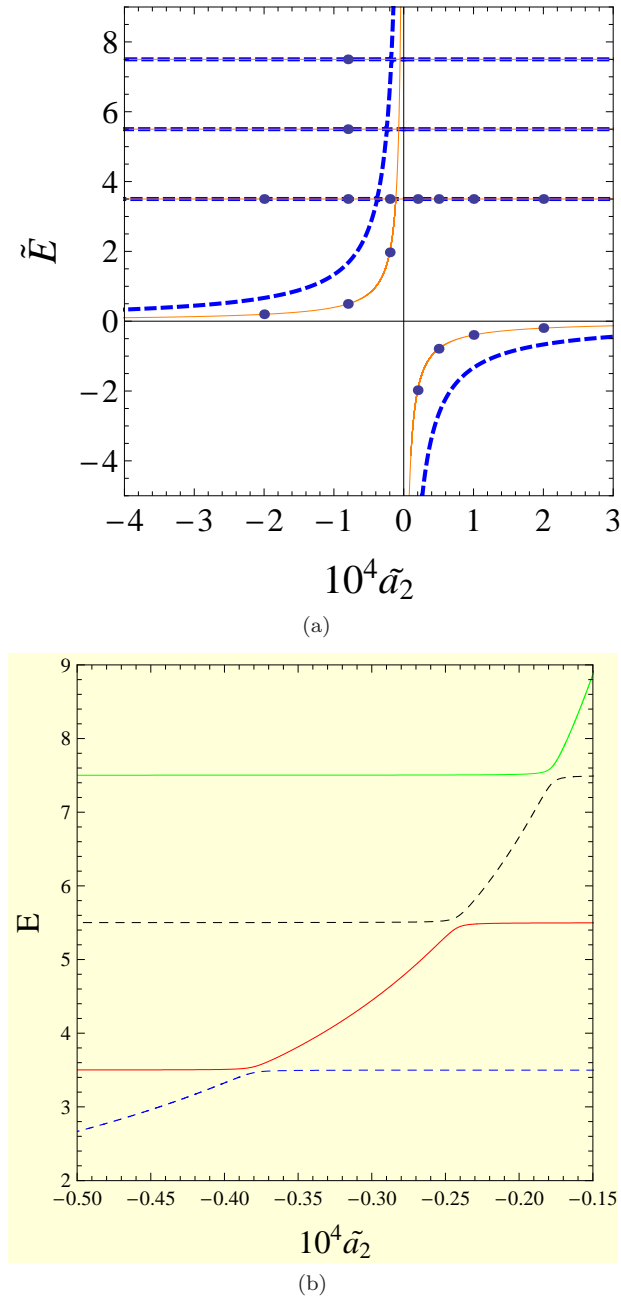


FIG. 3: (Color online) (a): The $l = 2$ energy levels vs the scaled d -wave scattering length. The dashed line is for $\tilde{r}_2 = -15 \times 10^3$, while the continuous line is for $\tilde{r}_2 = -15^4$. For the excited states, the dashed and continuous lines cannot be distinguished on this scale. See text for the choice of the effective range parameters. The superimposed dots are the numerically calculated energies obtained by solving the eigenvalue equation (6) directly. (b): Amplified version for the excited states showing that the levels do not actually cross, but bend sharply in Fig 3a.

Figs. (1-3) show that away from the resonance ($\tilde{a}_l \rightarrow \pm\infty$), the energy plots against \tilde{a}_l have similar shapes. But whereas the $l = 0$ plots remain essentially unchanged when \tilde{r}_0 is varied over a wide range, the higher partial

waves become more and more sensitive to the choice of the effective range. This is apparent from Figs.2-3. In all three, the lowest energy state tends to $-\infty$ as $\tilde{a}_l \rightarrow 0$. When $\tilde{a}_l \rightarrow \pm\infty$, the $l = 0$ energy levels tend to the limit $(2n + 1/2)$, $n = 0, 1, 2..$ in units of the oscillator spacing. By contrast, for $l \neq 0$, all but the lowest energy level go to the noninteracting values $(2n + l + 3/2)$ in the zero range limit. All energies are in units of the oscillator spacing. At resonance, the lowest energy level for $l \neq 0$ tends to zero as the range of the potential is decreased.

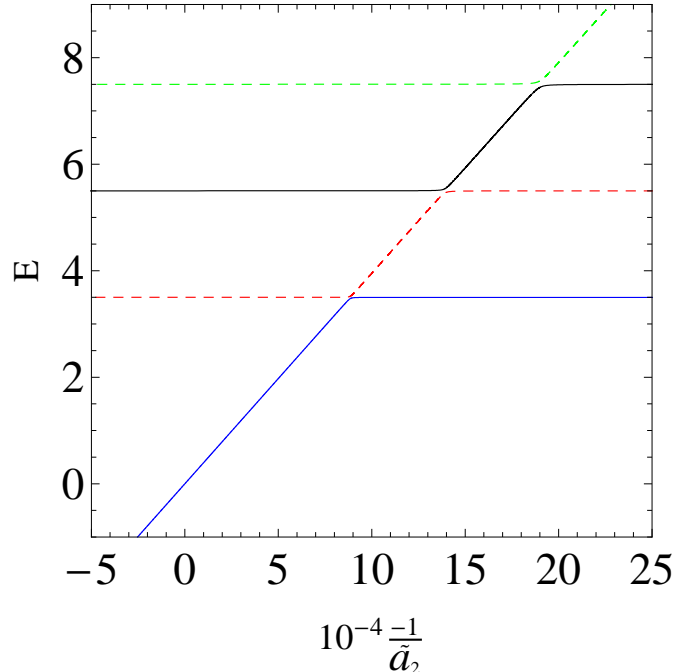


FIG. 4: (Color online) Plot of the excited state $l = 2$ energy levels vs the inverse of the scattering length in dimensionless units. This figure should be compared to Fig. 3 b.

In Fig. 4, we see that the higher energy levels show strong bends away from the resonance, a feature even more pronounced than for the $l = 1$ case shown in [9].

To confirm that the analytical result (18) does produce the energy spectrum for $l = 2$ accurately for the range of the scattering parameters shown in Fig. 3(a), we solved Eq.(6) numerically to determine η_2 . For V_s , a square-well potential was taken with $\tilde{b} = 1/15$, and it was kept fixed. The scattering length \tilde{a}_2 was varied as shown by changing the depth of the potential. In Fig. 3(a), the dashed curves and lines are plotted using the analytical formula (18). The superposed dots show the results for the eigenvalues obtained by the numerical integration of Eq.(6). The agreement is excellent, confirming the expectation of Appendix A. Table 1 shows, however, that the agreement with numerical integration becomes poor for the ground state as its energy approaches zero for large values of \tilde{a}_2 . This limitation is understandable from Eq.(24) derived in Appendix A and the discussion that follows it.

TABLE I: Comparison of energy η_2 obtained numerically from Eq.(6) and from the analytical formula (18). The range \tilde{b} of the square-well potential is kept fixed at $1/15$

$l = 2$	$10^4 \tilde{a}_2$		-2	-0.8	-0.2	0.2	0.5	1	2	100	10^5	10^8
$\tilde{E}(\hbar\omega)$	Ground state	N ^a	0.1992	0.4952	1.9726	-1.9772	-0.7887	-0.3945	-0.1956	-0.0022	0.0017	0.0017
		A ^b	0.1975	0.4939	1.9762	-1.9731	-0.7894	-0.3951	-0.1976	-0.0040	-0.0001	-0.0001
	First excited state	N	3.5002	3.5010	3.5012	3.5001	3.5001	3.5001	3.5002	3.5002	3.5002	3.5002
		A	3.5002	3.5002	3.5003	3.5001	3.5001	3.5001	3.5002	3.5002	3.5002	3.5002

^aNumeric results

^bAnalytical results

In summary, we have argued in this paper that it is legitimate to use the effective range formalism for higher partial waves in the presence of a coupling to a Feshbach resonance, even though these parameters may not exist for a long range $1/r^6$ interatomic potential. Next, we have derived an equation (18), valid *under certain restrictions* for any partial wave, relating the eigenenergies to the effective range parameters. This is known to be valid for $l = 0$ and $l = 1$ as long as the range of the potential is much shorter than the oscillator length. We have shown in this paper that it is also applicable for $l = 2$, so long as the ground state energy is not too close to zero. Our Eq.(24), derived for the matching distance for $l = 2$ shows the limitation of the shape-independent parameters. At resonance, since both the terms on the RHS vanish, the analytical result (18) becomes of limited validity. For $l > 2$, the restrictions are more severe.

We are indebted to Dr.Takahiko Miyakawa for many useful discussions at Tokyo University of Science (TUS), where much of the work was done. We would also like to thank the referee for the incisive comments that resulted in our adding Appendix A, and a deeper understanding

of the limitations of universality for $l \geq 2$. This work was supported by NSERC (Canada), and a grant from (TUS).

IV. APPENDIX

A. Appendix A

The energy spectrum Eq.(18) resulted when the ratio c'_2/c'_1 from (7) with the oscillator potential present was equated to the corresponding ratio from the scattering solution (14) without the confining potential. In doing so, we assumed that this matching was done at a small enough distance (still larger than the range b of $V_s(r)$) that the oscillator potential could be neglected. In this appendix, we justify this assumption by taking the specific example of $l = 2$. To do this, we need to write Eq.(16) in more detail, and examine the neglected terms in the expansion of Eq.(7). For $l = 2$, for small x , this is given by

$$u_2(x) = c'_1 \left[x^3 - \frac{\eta_2}{4} x^5 + \dots + \frac{c'_2}{c'_1} \left(x^{-2} + \frac{\eta_2}{6} + \frac{1}{24}(\eta_2^2 - 6)x^2 + \dots \right) \right]. \quad (21)$$

It is in the coefficient $\frac{(\eta_2^2 - 6)}{24}$ of the x^2 term that the oscillator presence is felt; without the oscillator, this coefficient is $\frac{\eta_2^2}{24}$. In Eq.(16), we neglect this term of order x^2 , and yet retain the leading term x^3 of the regular solution, even though x is small. This can only be justified if the matching distance x satisfies the inequality

$$x^3 \gg \left| \frac{c'_2}{c'_1} \right| \frac{x^2}{4}. \quad (22)$$

To check this, we substitute above the expression (17) for c'_2/c'_1 , which, for $l = 2$, gives the condition

$$x \gg \frac{45 |\tan \delta_2|}{4 (\sqrt{2}kL)^5}. \quad (23)$$

To estimate the RHS, we use Eq.(1), and put $k^2 = \frac{M}{\hbar^2} E_2$. We then get, for the condition (22)

$$x \gg 2 \left| \left(-\frac{1}{\tilde{a}_2} + \frac{1}{2} \tilde{r}_2 \frac{E_2}{\hbar\omega} \right)^{-1} \right|. \quad (24)$$

From Figs.3 and 4, we see that $\frac{1}{\tilde{a}_2}$ is of the order of 10^4 (either sign), and \tilde{r}_2 is -15×10^3 or ten times larger. The energy $E_2/\hbar\omega$ is of order unity. Unless there is some accidental cancellation, the RHS of Eq.(24) is very small, of the order of 10^{-4} . On the LHS of Eq.(24), x stands for the matching distance (in units of L , which is slightly larger than $\tilde{b} = 1/15$). Therefore the inequality condition (24) is easily satisfied when the scattering length \tilde{a}_2 is small. This is not the case at resonance, however,

when \tilde{a}_2 tends to infinity, and E_2 for the ground state approaches zero. We then see that the RHS of Eq.(24) tends to infinity, and the inequality condition cannot be satisfied. Our formula (18) is no longer accurate for the ground state in this situation. This is confirmed by our numerical calculation as shown in Table 1.

B. Appendix B

Consider an attractive square-well potential of depth V_0 and range b . Define the strength parameter

$$s = (\sqrt{MV_0/\hbar^2}) b. \quad (25)$$

In a given partial wave l , the expressions for the scattering length a_l and the effective range r_l are given by

$$a_l = -\frac{b^{2l+1}}{(2l-1)!!(2l+1)!!} \frac{j_{l+1}(s)}{j_{l-1}(s)}, \quad (26)$$

$$r_l = \frac{(2l-1)!!(2l+1)!!}{b^{2l-1}} \left[-\frac{1}{2l-1} + \frac{2l+1}{s^2} \frac{j_{l-1}(s)}{j_{l+1}(s)} - \frac{1}{2l+3} \left(\frac{j_{l-1}(s)}{j_{l+1}(s)} \right)^2 \right]. \quad (27)$$

-
- [1] C. A. Regal, C. Ticknor, J. L. Bohn, and D. S. Jin, Phys. Rev. Lett. **90**, 053201 (2003).
 - [2] A. Marte *et al.*, Phys. Rev. Lett. **89**, 283202 (2002).
 - [3] S. Inouye *et al.*, Nature (London) **392**, 151 (1998); Ph. Courteille *et al.*, Phys. Rev. Lett **81**, 69 (1998).
 - [4] T. Loftus, C. A. Regal, C. Ticknor, and D. S. Jin, Phys. Rev. Lett. **88**, 173201 (2002).
 - [5] T. Busch, B-G Englert, K. Rzazewski and M. Wilkens, Foundations of Physics, **28**, 549-559 (1998).
 - [6] S. Jonsell, Few-body Systems **31**, 255-260 (2002).
 - [7] P. Shea, B. P. van Zyl, and R. K. Bhaduri, Am.J.Phys. (in press) 2009.
 - [8] T. Stöferle *et al.*, Phys. Rev. Lett. **96**, 030401 (2006).
 - [9] S.-K. Yip, Phys. Rev. **A78**, 013612 (2008).
 - [10] C. Ticknor, C. A. Regal, D. S. Jin, and J. L. Bohn, Phys. Rev. **A69**, 042712 (2004).
 - [11] S.-K. Yip, arXiv:0801.0636v1 (unpublished).
 - [12] N. F. Mott and H. S. W. Massey, *The Theory of Atomic Collisions* (Oxford University Press, Third Edition, 1965) p.50.
 - [13] L. D. Landau and E. M. Lifshitz, *Quantum Mechanics*, (Addison-Wesley, Reading, Massachusetts) (1958), p.405.
 - [14] Bo Gao, Phys. Rev. **A58**, 4222 (1998).
 - [15] T. Köhler, K. Goral and P. S. Julienne, Rev. Mod. Phys. **78** 1311 (2008) .
 - [16] M. Block and M. Holthaus, Phys. Rev. **A65** 052102-1 052102-4 (2002).
 - [17] C. Cohen-Tannoudji, in *Lectures on Quantum gases*, Institut Henri Poincare, Paris, April 2007 (unpublished). PDF available at <http://www.phys.ens.fr/~castin/progtot.html>.
 - [18] B. R. Levy and J. B. Keller, J. Math. Phys. **4**, 54 (1963).